Nanoscale

Accepted Manuscript

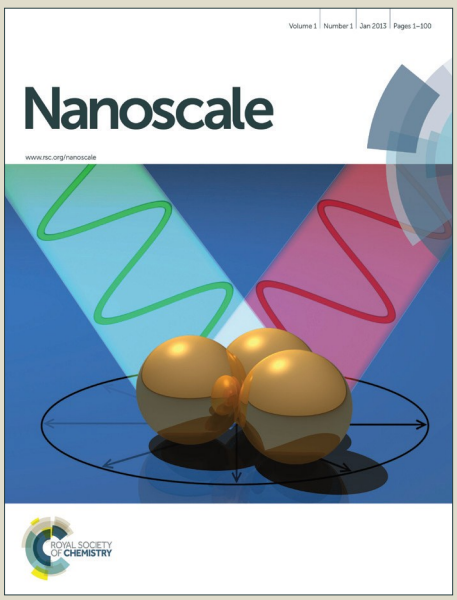

ROYAL SOCIETY OF CHEMISTRY

www.rsc.org/nanoscale

Nanoscale

RSCPublishing

ARTICLE

Controlled implant/soft tissue interaction by nanoscale surface modifications of 3D porous titanium implants

Cite this: DOI: 10.1039/x0xx00000x

Received 00th January 2012,
Accepted 00th January 2012

DOI: 10.1039/x0xx00000x

www.rsc.org/

Elisabeth Rieger [a,b,c], Agnès Dupret-Bories [a,c,d], Laetitia Salou[e,f], Marie-Helene Metz-Boutigue[a,b], Pierre Layrolle[e], Christian Debry [a,c], Philippe Lavalle[a,b], Nihal Engin Vrana[a,g*]

Porous titanium implants are widely employed in orthopaedics field to ensure good bone fixation. Recently, the use of porous titanium implants has also been investigated in artificial larynx development in a clinical setting. Such uses necessitate a better understanding of the interaction of soft tissues with porous titanium structures. Moreover, surface treatments of titanium have been generally evaluated in planar structures while the porous titanium implants have complex 3 dimensional (3D) architectures. In this study, the determining factors of soft tissue integration of 3D porous titanium implants were investigated as a function of surface treatments via quantification of the interaction of serum proteins and cells with single titanium microbeads (300-500 µm in diameter). Samples were either acid etched or nanostructured by anodization. When the samples are used in 3D configuration (porous titanium discs of 2 mm thickness) *in vivo* (in subcutis of rats for 2 weeks), a better integration was observed for both anodized and acid etched samples compared to the non-treated implants. If the implants were also pre-treated with rat serum before implantation, the integration was further facilitated. In order to understand the underlying reasons for this effect; human fibroblast cell culture tests under several conditions (directly on beads, beads in suspension, beads encapsulated in gelatin hydrogels) were conducted to mimic the different interactions of cells with Ti implants *in vivo*. Physical characterization showed that surface treatments increased hydrophilicity, protein adsorption and roughness. Surface treatments also resulted in improved adsorption of serum albumin which in turn facilitated the adsorption of other proteins such as Apolipoprotein as quantified by protein sequencing. The cellular response to the beads showed considerable difference with respect to the cell culture configuration. When the titanium microbeads were entrapped in cell-laden gelatin hydrogels, significantly more cells migrated towards the acid etched beads. In conclusion, the nanoscale surface treatment of 3D porous titanium structures can modulate *in vivo* integration by the accumulative effect of the surface treatment on several physical factors such as protein absorption, surface hydrophilicity and surface roughness. The improved protein adsorption capacity of the treated implants can be further exploited by a pre-treatment with autologous serum to render the implant surface more bioactive. Titanium microbeads are a good model system to observe these effects in a 3D microenvironment and provide a better representation of cellular responses in 3D.

Keywords: Titanium; soft tissue; acid etching; anodization; surface treatment; *in vivo* test; tracheal prosthesis

A Introduction

Titanium is a commonly used biomaterial especially in hard tissue replacement applications [1]. Most of the studies on titanium focused on its interaction with bone tissue cells or stem cells with an aim to convert them to osteoblasts. However recently there have been attempts to use titanium implants in other medical indications, particularly for tracheal replacement [2-5]. These efforts necessitate a better understanding of the interaction of titanium surfaces with soft tissues. The behaviour of different cell types in contact with titanium can be distinctly different. One such example is the interaction of gingival epithelial cells with dental titanium implants where epithelial cells prefer polished titanium to sandblasted titanium[6]. Cell/implant interactions have another aspect in otorhinolaryngology, as unlike in the case of dental implants where most of the patients are healthy otherwise, the tracheal implants are designed particularly for patients with recent cancer and surgical history. Hence, it is even more important to optimize surface properties for improved implant tissue integration.

We have recently reported the first successful clinical application of a titanium based artificial larynx system after total laryngectomy [7]. Removal of larynx is a necessity for late stage laryngeal cancer patients and it results in considerable problems for the patient due to the presence of a tracheostomy (the trachea is attached to the skin of the neck to re-establish breathing.). The most important consequences are due to the shunt of the aerodigestive upper way: breathing with the tracheostomy (and not with the nose or the mouth), and difficulties in speaking (the patient has to learn oesophageal voice, or a small valve between the trachea and the oesophagus can be placed during the surgery). An artificial larynx system that can replace the functions of the larynx after total larynx resection would significantly improve the life quality of these patients. A system composed of a removable valve system and a permanent titanium implant part (ENTegral®, Protip

Medical), can restore several functions of larynx and provides the patient with a means to breathe without a tracheostomy. Titanium was selected because the mechanical properties of titanium prevent the possible collapse of the airway, which is a common risk in tracheal implants. In order to ensure the proper integration between the implant and the trachea, a macroporous, microbead based system was utilized. However, due to the physical properties of the titanium, the connection between the titanium and the surrounding tissue might not be rapidly established. This would further lengthen the inflammatory process. Thus, it is important to mediate the interaction of the implant with the surrounding soft tissue via surface modifications without compromising the bulk properties of the implant.

Surface properties are the most dominant aspect of non-degradable, implantable biomaterials [8] and are widely used to improve metallic implant's bioactivity. For example, it has been shown that acid etching of orthopaedic implants resulted in better osseointegration as quantified by the increased torque force to remove the implants *in vivo*[9]. Many methods, such as hydroxyapatite coating, polymer adsorption, etching, covalent bonding, anodization have been used to achieve beneficial effects [10, 11]. However quantification of these effects is generally limited to 2D, planar surfaces. This approach cannot fully capture the possible *in vivo* outcomes for complex implants, particularly porous implants. Moreover, all these modifications simultaneously change several parameters such as surface roughness, hydrophilicity and protein adsorption capacity, which makes it even harder to pinpoint the exact reasons behind the improvements in cellular behaviour.

In dental implants field, the general understanding is that a rough titanium surface is better for bone attachment whereas a smooth surface helps the gingival fibroblast adhesion. However, these conclusions are based on a structure where the interaction of the cells with the implant surface is planar. How the surface properties of titanium in a 3D configuration affect the cellular interaction with the implant surface is still an open question. These effects are difficult to quantify in metal

foams as the pore shapes are irregular and the distribution of the pore sizes is widespread. Thus a model in which the geometrical control over the components of the porous structure can be achieved, is desirable.

Microbead based macroporous titanium implants (Figure S1), provide a 3D system where it is possible to study the effects of surface modification on the building blocks of the system[12]. We have recently shown that just by changing the size of microbeads extensive changes in the *in vivo* integration process can be obtained [13]. It has been previously shown that Hydrochloric acid (HCl) etching of porous titanium implants improves their osseoinductivity [14]. Also effects of anodization on osseointegration and osteogenic differentiation of mesenchymal stem cells have been demonstrated [15, 16]. In this study, the effects of the surface modifications on *in vivo* soft tissue migration into the porous implants were observed by a rat subcutaneous implantation model for 2 weeks. In order to elucidate the reasons for the beneficial effects of nanoscale surface treatments on *in vivo* integration, we have used single titanium microbeads of 300-500 μm in diameter to study the effect of surface modifications on human fibroblast cell behaviour with respect to several parameters which are known to effect cell attachment, namely surface hydrophilicity, roughness and serum protein adsorption. The nature and the content of proteins adsorbed was quantified by High performance liquid chromotography (HPLC) separation and subsequent protein sequencing to better understand the interaction between surface property changes and protein retention. Different cell culture configurations were used to mimic different *in vivo* conditions, such as mimicking cell in-growth from surrounding soft tissues by encapsulation of single titanium beads in cell-laden gelatin hydrogels.

B Results and Discussion

Results

The surface treatments had profound effects on the integration of the implants *in vivo* (Figure S2). After two weeks of subcutaneous implantation in rats, the extent of tissue formation around the implants was considerably higher in surface treated samples. Scanning Electron Microscope (SEM) images demonstrated that both on the surface and in the cross-section; there was considerably more cell presence and extracellular matrix deposition for both anodized and HCl treated samples (Figure 1). Particularly, the amount of tissue in the cross-section was significantly higher ($p<0.05$). We also observed an increased expression of Interleukin-10 (IL-10) and Tissue Inhibitor of Matrix Metalloprotease 1(TIMP-1) by Reverse transcription Polymerase chain reaction (RT-PCR) in anodized samples which are anti-inflammatory markers, whereas there was no significant difference in the expression of the other genes checked between the groups. We also tried the introduction of rat serum onto the implants prior to the implantation as a means to induce protein adsorption and subsequent facilitation of the tissue integration. This treatment not only improved the colonization of non-treated implants but resulted in additional amelioration for the treated surfaces, with significantly more colonization (Figure 2). When the total area covered by tissue for both the surface and the cross-section of the implants were quantified, we observed that the treated implants had significantly more coverage in all configurations ($p<0.05$) (Figure 3). Also, in treated samples there was a significantly higher amount of collagen secretion (Figure S3).

Figure 1. SEM micrographs of explanted porous titanium implants after subcutaneous implantation.

Figure 2. SEM micrographs of explanted porous titanium implants after subcutaneous implantation with prior rat serum treatment.

Figure 3. Quantification of the tissue coverage of the explanted implants with image analysis. Surface treatments resulted in a significantly higher coverage particularly in the cross-section ($p < 0.05$).

Figure 4. SEM micrographs. Surface morphology of single titanium beads after surface treatments.

Anodization locally induced microlevel changes but its effect was mainly at nanometer level with production of a regular array of titanium oxide nanotubes (Figure S4). The size of nanotubes were 50±16 nm; having a size suitable for deposition of proteins. We have selected HCl etching due to the milder conditions of etching (Figure 4). Utilization of different acids led to different surface morphologies for the beads, for example Hydrofluoric acid (HF) resulted in considerable change in bead morphology within a short period (90 s) whereas HCl and Sulfuric acid (H_2SO_4) treatments where mainly limited to the surface changes (Figure S5).

The topographical changes observed caused an increase in the roughness of the surfaces. As in the case of morphological changes, HF (R_a=82.4±14.8 nm) and H_2SO_4 (R_a= 43.6±30.4 nm) treatments cause rougher surfaces whereas HCL (R_a=17.5±6.0 nm) and anodization (R_a= 16.4±2.6 nm) only resulted in slight but significant increases in surface roughness (compared to the roughness of untreated titanium (R_a=8.4±0.3 nm); however it should be noted that the nanotubes are closely packed with a diameter which is difficult to visualize with Atomic Force Microscopy (AFM). This might be the reason of the small change in roughness for anodized samples (Figure 5).

Figure 5. AFM micrographs and surface roughness. Effect of different surface treatments on the surface topography and roughness of the titanium beads.

Surface treatments improved the hydrophilicity of pure titanium which had a contact angle of 66.2 ± 3.6 º. Both anodization and acid etching decreased the contact angle, i.e. increased the hydrophilicity (Figure S6). This had a direct effect on protein adsorption on the microbeads also. We have quantified the adsorption of proteins from human serum. When human serum was directly used, acid etched samples adsorbed more proteins as quantified by HPLC. (Figure 6). The main proteins that have been adsorbed were Albumin, Transferrin, Apolipoprotein A, Alpha 1 antitrypsine and vitamin D binding protein. After depletion of IgG and Albumin, again there was a significant difference in the absorption of Apolipoprotein and Alpha 1 antitrypsine. For anodized samples the absorption trend was similar although the adsorption was less compared to HCl treated surfaces.

When the beads are placed on Tissue culture polystyrene (TCPS), there was no statistical difference in the attachment of cells between different treatments (Figure 7a); however when the beads are placed on non-cell adhesive surfaces treated beads attracted significantly more cells ($p<0.05$) (Figure 7b). In the case of encapsulated cells, presence of the beads had no cytotoxic effect so the cell numbers were comparable (Figure 7c); but the cells over 5 days preferred to move towards treated beads compared to non-treated beads.

Figure 6. HPLC and Protein Sequencing. Comparison of the human serum before and after being in contact with the treated or non-treated Titanium beads and the main proteins adsorbed from the serum.

Figure 7. Attachment of Human Gingival Fibroblasts (HGF) to treated or non-treated beads and effect of bead presence on cell viability within gelatin hydrogels.

After 5 days of culture, the surface of the treated beads were mostly covered by cells in suspension culture whereas the non-treated beads had less cells due to the lack of initial attachment (Figure 8a). For gel culture, cells preferentially moved towards the beads; most probably due to its stiffness. This cell migration was more pronounced in the cases of anodized and HCl treated beads (Figure 8b). In the case of TCPS surfaces, the cells became confluent and the beads were covered for all cases (Figure 8c). When analysed with confocal microscopy the superior cell coverage on treated samples were more apparent for all conditions except TCPS (Figure 9).

Figure 8. FM micrographs. Hoechst/Phalloidin/Vimentin staining of cells after 5 days of culture under 3 different culture configurations. Scale bar = 100 μm.

Figure 9. Confocal micrographs. 3D reconstruction of HGF cells cultured on titanium beads in different configurations. Scale bar = 100 μm.

Discussion

One of the primary effects of both etching and anodization is the alteration of titanium surface topography at both nano- and micro levels. Topographical changes even at the level of 10 nm can affect cell behaviour. It has been recently shown that the presence of surface micro- and nanotopographies can downregulate inflammatory response [17] with a significant decrease in both polymorphonuclear and mononuclear cells in rat subcutaneous implantation experiments. The decrease in the initial response due to the surface structuration might contribute to the faster

integration of 3D porous structures too. For stem cells, it has been shown that the presence of nanoscale cues might be enough by itself for successful commitment of cells to a specific differentiated cell type [18]. Nanoscale cues can also provide surfaces with different preference to bacterial and mammalian cell attachment [19]. For osteoblasts, the positive effect of both acid etching and anodization is well recorded and a recent study showed that while both anodized and acid etched surfaces resulted in up-regulation of osteoblast differentiation related genes, anodized surfaces also caused an increase in cell adhesion related genes [20]. Thus the presence of the nanoscale cues on the surfaces of the titanium beads can provide a better surface for cell attachment.

At the coating level, it has been shown that rough titanium surfaces can decrease fibroblast activity while increasing osteoblast activity [21]. But for bulk materials, especially surface modified materials, the effect is not only related to the roughness, thus the fibroblast behaviour is more varied. For example, as the roughness results for the acid etched and anodized beads shows before and after serum incubation, the changes in surface topography affects the protein adsorption and protein adsorption in return affects the surface roughness. For HCl etched beads due to the increased protein adsorption there was an increase in the surface roughness, whereas most probably due to the filling of the nanotubes the effect was reversed for anodized samples. These might result in differential integrin clustering due to the distribution of the proteins on the implant surface. But even though the anodized samples have lower protein adsorption and roughness compared to acid etched samples, the size of the nanotubes exert additional and more precise effects on cell/surface interaction. Also, the anodisation directly forms the nanotubes in the surface Titanium oxide layer, whereas acid etching, physically etches the surface, which then forms an oxide layer upon contact with air. The protein absorption process goes through the filling of the nanotubes and it has been shown that with pores greater than 100 nm this may not be

achieved; but for pores of 50 nm they can be completely filled [22]. Also it should be noted that the due to the movement restrictions of the AFM tip the roughness of anodized samples can be lower than their actual values.

The method and nature of nano/micro structuration is also an important determinant. For example laser assisted structuration methods can result in highly hydrophobic surfaces, even though the surface is highly hydrophilic immediately after the treatment [23], due to the regular nature of the surface topography, without a chemical change at the interface level (where the chemical effect of the treatment is only applicable in the direct treatment areas with the laser). The effect of surface treatment on surface hydrophilicity is also treatment dependent, the hydrophobicity of untreated titanium surfaces is largely due to the presence of contaminants and both acid etching and anodization can remove them[24]. Dynamic contact angle analysis of microstructured titanium surfaces has shown an improved wettability following the first immersion cycle[25]. Thus, it is not feasible to describe the biological activity of the surface with respect to its initial contact angle. For the bulk materials, protein adsorption seems to be a more determinant factor than surface roughness. For example, if the roughness is obtained by grounding the reverse effect and improved fibroblast response has been reported [26]. Moreover, in a planar surface it is easier to single out the effect of roughness as the cells only interact with the surface from the top. For human gingival fibroblasts, formation of a hydride layer was shown to be an effective way of improving attachment [27], however again it was not possible to distinguish the source of this effect with respect to surface roughness or contact angle. It was suggested that the effect of the hydride layer is to improve the protein adsorption. In this study we have also shown that the surface treatments are able to increase the protein adsorption on the porous titanium surfaces. The quantification of the specific proteins that are preferentially adsorbed to a given surface can control the initial phases of tissue response to the implant [28]. Formation of an initial serum

albumin layer on implants is a common occurrence due to the relative abundance of serum albumin. *In vitro* this can decrease the adsorption of less abundant proteins like fibronectin, vitronectin which are more relevant for cell attachment. However, the extent of this initial layer can facilitate the adsorption of other proteins *in vivo*, thus a higher serum albumin adsorption can be advantageous, as in the case of treated surfaces in this study. For example, one of the proteins identified in this study, Apolipoprotein, has been implicated in having an effect in regeneration and also in cell growth and proliferation [29], but it has been also related to inhibition of endothelial cell growth. Whereas, Alpha 1 Antitrypsin is a protease inhibitor that can increase the retention time of the other adsorbed proteins due to its anti-protease activity [30].

Most of the studies on the effect of surface properties on cells are done on planar surfaces which are hard to convert into information in 3D configurations. In a 3D metallic foams cells are exposed to significantly curved surfaces which has been shown to effect their ability to move and spread by affecting the contractile forces exerted by the cell cytoskeleton [31]. Moreover, analysis of the 3D titanium structures especially with conventional methods is difficult. Titanium microbeads are small enough to be visualized by fluorescence microscopy or confocal microscopy, which provides an opportunity to observe the cellular behaviour in a more 3D microenvironment. Moreover, bead based structures are advantageous as they provide macroscopically smooth surfaces that interact with the surrounding tissue unlike many metallic foams which has sharp edges that can damage the tissues in vicinity. Also physical properties such as porosity or pore size can be easily modified by using the mixture of beads with different granulometry. Previously polymeric beads has been used in delivery and immunoisolation of the cells as they provide an excellent surface:volume ratio and a beneficial effect on mass transfer limitations [32]. As our clinical practice showed that 3D structures composed of titanium microbeads can be integrated

easily *in vivo*, 3D microbead-based titanium structures can be beneficial for filing load-bearing defects with an openly porous material with good mechanical properties.

The effects of surface treatments *in vivo* were much more pronounced compared to *in vitro* results. This is due to the incremental effects of increased hydrophilicity and roughness and resulting protein adsorption. As the biomaterial interaction with the body is mainly governed by the initial interaction with the body fluids, mainly blood, and subsequent protein adsorption it is important for *in vivo* application to utilize this interactions beforehand. The blood in the surgery area is in direct contact with wounded endothelial cells and will most probably contain high amounts of pro-inflammatory signals; thus its adsorption on the surface of the implant not only will trigger coagulation but also will result in a more pro-inflammatory initial response. However, if the implant has already been partially coated with autologous serum from peripheral blood; then this effect can be diminished. As the surface treatments increase the protein adsorption this would be a good way to boost the colonization also. Our *in vivo* tests showed that for all conditions application of serum caused a significant increase in colonization.

C Experimental

C 1 Materials.

Pure Medical Grade Titanium beads (Ti40) were purchased from Neyco SA (Paris, France). All chemicals were purchased from Sigma-Aldrich (Germany) unless otherwise stated. Primary Vimentin antibody was purchased from Santa-Cruz (California, USA). Vybrant cell adhesion assay was purchased from Life Technologies (USA). RNeasy mRNA extraction kit was purchased from Qiagen (The Netherlands) and iScript Reverse transcription Supermix for RT-qPCR was obtained from Bio-Rad. Apoptotic/Necrotic/Live cell assay was purchased from PromoKine (Heidelberg, Germany).

C 2 Methods

C 2.1 Surface Treatments

Surface modification of the single titanium beads, plain titanium and 3D porous titanium samples (discs of 10 mm diameter and 2 mm of thickness) were done as described below (Table 1). For anodized samples an annealing treatment for 1h at 500 °C was carried out to stabilize the nanotubes. After the treatments samples were washed with distilled water and air-dried.

Table 1. Titanium Surface Treatments.

C 2.2 In vivo tests

9 male Wistar rats weighing 300g were implanted. Approval for these experiments was obtained from the Regional Commitee of Ethics for Animal Experiments of Strasbourg. The implantation procedure was done under general anaesthesia, obtained with intra peritoneal injection of a mixture made with 90 mg/kg of ketamine and 10 mg/kg of xylazine. Local anaesthesia of the skin of the back was performed (1% lidocaine). Implants were put subcutaneously in the back of the animals. The skin was stitched up with several stitches. Each animal except one received four implants two at each side of the spinal column, where one side has the treated implants while the other side has the controls). In total 6 implants for each condition without serum treatment and 3 implants for each condition with serum treatment were implanted. Animals were daily observed to ensure their well-being and whether there were any signs of infection at the operation area. Two weeks after implantation procedure, animals were anaesthetised and the implants were explanted. Macrophotographies of the implants were done and fixed in 4% Formol for 24 hours. Cross-sections of the implants were obtained by freeze-etching using liquid nitrogen. Afterwards, implants were coated with a 10 nm gold layer to be observed with SEM, the total coverage after 2

weeks for surface and cross-section for each condition was quantified using Image J image analysis program. Total amount of protein and collagen were quantified by semi-quantitative Fast Green-Sirius Red staining. Explants with the in-grown tissue were immersed in 30 mg/ml protease solution in sterile MilliQ water (Origin of protease was Streptomyces griseus). For total digestion of the in-grown tissues, up to 48 hours of incubation was necessary. mRNA was achieved by RNeasy kit as per instructions of the provider. The amount of extracted RNA and its quality were measured by a Nanodrop spectrometer system (Thermo Scientific). The reverse transcription of the complementary DNA was done by Reverse transcription Supermix for RT-qPCR (Bio-Rad), by the following cycle configuration: 5 min at 25°C, 30 min at 42°C and 5 min at 85°C. The PCR amplication was done with the following reaction solution composition: 4 µL de supermix at 5 M, 0,1 µL of forward primer 0,1 µL of reverse primer, 0,2 µL of Taq polymerase (iTaq DNA polymerase, Bio-Rad), 4 µL of Betaine at 5 M, 1 µL of DMSO, 9,6 µL filtred MilliQ water and 1 µL complementary DNA. The amplification cycle was as follows: 1 min at 94°C, 1 min at 60°C, then 1 min at 72°C for 35 times. The primers were designed by the primer design tool of the primer provider (Eurofins MWG, Operon).The expression level of the following genes were checked: Interleukin-10 (IL-10), Tissue inhibitor of Matrix metalloprotease 1(TIMP-1), von Willebrand factor (vwf), Vascular endothelial growth factor A (VEGF A), Tumor necrosis factor alpha (TNF-α), Cadherin 1 (Cdh-1), Vascular Cell Adhesion Molecule 1 (VCAM-1), Interferon gamma (IF-γ), Transforming Growth Factor beta (TGF-ß1), Glyceraldehyde-3-phosphate dehydrogenase (Gapdh), beta actin (ß-actin) with the aim of comparing if there is a significant difference in the pro and/or anti-inflammatory and vascularisation related markers.

C 2.3 Surface Characterization

The surfaces of the titanium beads were characterized for the morphology, roughness, topography and surface hydrophilicity. Effect of the treatment on bead morphology was characterized by visualization of single beads by Scanning Electron Microscopy (SEM, Hitachi TM-1000). The effect of the treatments on surface roughness was quantified by AFM in contact mode in 10 micron x 10 micron fields (Multimode Nanoscope VI , Bruker (Santa Barbara, CA, USA)). Surface roughness was calculated from an average of 6 images. Contact angles of the treated and non-treated surfaces were done by the measurement of contact angle for a 10 microliter water droplet. Protein adsorption was initially quantified by BCA assay and further characterization was done as described below.

C 2.4 Quantification of Serum Protein ADsorption via HPLC and Sequencing

In order to quantify the amount of protein adsorbed, single beads (which corresponds to a ~ 8x 10^5 μm^2 surface area with an average bead diameter of 500 μm) of each condition were incubated in human serum at room temperature for 1 hour. After the incubation the serum was removed and introduced to the HPLC system to quantify the missing amount of protein components which have been adsorbed. For the baseline human serum was directly introduced into the HPLC system.

C 2.4.1 - RP-HPLC purification

The proteins present in samples (100 μL) were separated at 40°C using a Dionex HPLC system (Ultimate 3000; Sunnyvale, CA USA) on a Vydac 208TP C8- column (particle size, 5 μm ; 150 mm x 2.1 mm ; Grace, Vydac, Interchim, Montluçon, France) with a pre-column heater 2 μL and 0.13 mm for internal diameter (Interchim, Montluçon, France). Absorbance was monitored at 214 nm, and the solvent system consisted of 0.1% (v/v) TFA in water (solvent A) and 0.09% (v/v) TFA in 70% (v/v) acetonitrile-water (solvent B). Elution was performed at a flow rate of 200 μL/min with the following solvent B gradient : 0%B during 5 min, 0%B to 100%B during 45 min

and 100%B during 10 min. Fractions containing peaks were manually collected and concentrated until 20 µL by evaporation using a speed-vac.

C 2.4.2 Automatic Edman sequencing of peptides

The N-terminal sequence of purified peptides was determined by automatic Edman degradation analysis on a Procise bi-cartridge microsequencer (Applied Biosystems, Courtaboeuf, France). Samples purified by HPLC were loaded on polybrene-treated glass-fibre filters. Phenylthiohydantoin-amino acids (Pth-Xaas) were identified by chromatography on a C18 column (PTH C-18, 2.1 mm Å~ 200 mm) and comparison with the profile of the Pth-Xaas standard.

2.2.4.3 Identification of the isolated proteins

The sequence of the protein obtained after sequencing is compared with protein sequences included in the data bank UniProtKB by using http://web.expasy.org/blast/.

C 2.5 CELL CULTURE

Primary Human Gingival Fibroblasts isolated in University of Strasbourg Dental Faculty with patient consent were used at passage 3-6. The medium was DMEM low glucose with 10% Foetal Bovine Serum (FBS) and 1% Pen/Strep. Cells were passaged regularly and fed every other day. Trypsinized cells were seeded on single beads which are sterilized by UV treatment. For bead suspension experiments non-adhesive cell culture plates were used (NUNC). 1 x 10^5 cells were seeded on each bead. For encapsulation 5% porcine gelatin solution was used. 1.2 x 10^5 cells were encapsulated within the gel of 80 µl in 96 well plates which contains a single titanium bead inside by introduction of transglutaminase to crosslink gelatin (6:1 v:v ratio).

C 2.6 CELL CULTURE CONFIGURATIONS

Cell culture experiments were done in 3 configurations as described in Figure 10 in 96 well plates. First, to see the competitive attachment of the cells, cells were seeded on beads on TCPS

where they can attach both to the well and to the titanium bead. In the second configuration, to see the preference of the cells to attach on the beads, a non-adhesive plate was used, so that the cells can only attach to the beads. The third configuration was the encapsulation of the beads in a cell laden enzymatically degradable hydrogel (gelatin) to mimic the movement of the cells from the surrounding tissue to the implant.

Figure 10. The treatments and the Cell Culture configurations utilized.

C 2.7 Cell Viability, Morphology and Distribution

Initial cell attachment and viability over 5 days was tested with TOX-8 (A resazurin based cell metabolic activity test). Cellular morphology and cell distribution was either observed by Calcein-AM staining or Hoechst/Phalloidin/Vimentin staining. 3D imaging of single beads in every configuration was done by a confocal microscope after Calcein-AM staining. Total cell area and total cell numbers for each conditions were determined by Image-J image analysis program (NIH, USA)[33].

C 3 Statistical Analysis

The experiments are done at least in triplicates (For cell culture and protein adsorption in sextuplicates) and the results presented are the results of at least 3 independent experiments and they are reported as mean± SD. The comparisons between, non-treated, acid etched and anodized conditions was done by one-way ANOVA analysis at a statistical significance level of $p<0.05$, followed by Tukey's test to determine the differences in between samples.

Conclusions

The effects of two surface modification techniques, acid etching and nanotube formation via anodization, was quantified in a 3D model. The sum of all effects of surface treatments that are beneficial for cell attachment such as increased surface roughness, improved protein adsorption has been shown to have an exponential impact to the *in vivo* integration. The ability to test the single components of an implant *in vitro* to understand *in vivo* behaviour is an advantage of modular systems such as microbead-based porous titanium implants. These treatments will be tested for improvement of colonization of porous titanium tracheal connectors in artificial larynx implants.

Acknowledgements

This project has received funding from the European Union's Seventh Framework Programme for research, technological development and demonstration under grant agreement no. 606624 (NanoTi). This study has been partially funded by Protip Medical, Fédération de Médecine Translationnelle de Strasbourg (FMTS), Université de Strasbourg, France, and Ligue contre le cancer Alsace, France.

Notes and references

[a] *Institut National de la Santé et de la Recherche Médicale, INSERM Unité 1121, 11 Rue Humann, 67000 Strasbourg, France*

[b] *Faculté de Chirurgie Dentaire, Université de Strasbourg, 1 Place de l'Hôpital, 67000 Strasbourg, France*

[c] *Hôpitaux Universitaires de Strasbourg, Service Oto-Rhino-Laryngologie, 67098 Strasbourg, France*

[d] *Institut Universitaire du Cancer de Toulouse, 1 avenue Irène Joliot Curie 31059 Toulouse, France*

[e] *Inserm, UMR957, Lab. Pathophysiology of Bone Resorption, Faculty of Medicine, University of Nantes, France*[f] *Biomedical Tissues SAS, IRTUN, 8 Quai Moncusu, 44008 Nantes, France*[g] *Protip Medical, 8 Place de l'Hopital, 67000, Strasbourg, France*

**Corresponding Author: Dr. Nihal Engin Vrana*

Fax : +33 388329209 e-mail : e.vrana@protipmedical.com

Electronic Supplementary Information (ESI) available: [6 supplementary figures Figure S1-S6]. See DOI: 10.1039/b000000x/

1. J. P. Li, P. Habibovic, M. van den Doel, C. E. Wilson, J. R. de Wijn, C. A. van Blitterswijk and K. de Groot, *Biomaterials*, 2007, 28, 2810-2820.
2. N. E. Vrana, A. Dupret-Bories, C. Bach, C. Chaubaroux, C. Coraux, D. Vautier, F. Boulmedais, Y. Haikel, C. Debry, M.-H. Metz-Boutigue and P. Lavalle, *Biotechnology and Bioengineering*, 2012, n/a-n/a.
3. L. M. Janssen, G. J. V. M. van Osch, J. P. Li, N. Kops, K. de Groot, L. Feenstra and J. A. U. Hardillo, *Journal of Tissue Engineering and Regenerative Medicine*, 2010, 4, 395-403.
4. A. Dupret-Bories, P. Schultz, N. E. Vrana, P. Lavalle, D. Vautier and C. Debry, *Journal of Rehabilitation Research and Development*, 2011, 48, 851-863.
5. A. A. Gaafar, A. A. El-Daly and H. A. Gaafar, *The Journal of Laryngology & Otology*, 2008, 122, 391-396.

6. G. Lauer, M. Wiedmann-Al-Ahmad, J. E. Otten, U. Hübner, R. Schmelzeisen and W. Schilli, *Biomaterials*, 2001, 22, 2799-2809.

7. C. Debry, A. Dupret-Bories, N. E. Vrana, P. Hemar, P. Lavalle and P. Schultz, *Head & Neck*, 2014, n/a-n/a.

8. F. Variola, F. Vetrone, L. Richert, P. Jedrzejowski, J.-H. Yi, S. Zalzal, S. Clair, A. Sarkissian, D. F. Perepichka, J. D. Wuest, F. Rosei and A. Nanci, *Small*, 2009, 5, 996-1006.

9. S.-A. Cho and K.-T. Park, *Biomaterials*, 2003, 24, 3611-3617.

10. G. Zhao, Z. Schwartz, M. Wieland, F. Rupp, J. Geis-Gerstorfer, D. L. Cochran and B. D. Boyan, *Journal of Biomedical Materials Research Part A*, 2005, 74A, 49-58.

11. K. Mustafa, J. Wroblewski, B. S. Lopez, A. Wennerberg, K. Hultenby and K. Arvidson, *Clinical Oral Implants Research*, 2001, 12, 515-525.

12. N. E. Vrana, A. Dupret-Bories, C. Chaubaroux, E. Rieger, C. Debry, D. Vautier, M.-H. Metz-Boutigue and P. Lavalle, 2013, e50533.

13. N. E. Vrana, A. Dupret-Bories, P. Schultz, C. Debry, D. Vautier and P. Lavalle, *Advanced Healthcare Materials*, 2013, n/a-n/a.

14. M. Takemoto, S. Fujibayashi, M. Neo, J. Suzuki, T. Matsushita, T. Kokubo and T. Nakamura, *Biomaterials*, 2006, 27, 2682-2691.

15. S. Lavenus, M. Berreur, V. Trichet, P. Pilet, G. Louarn and P. Layrolle, *Eur Cell Mater*, 2011, 22, 84-96.

16. S. Lavenus, V. Trichet, S. Le Chevalier, A. Hoornaert, G. Louarn and P. Layrolle, *Nanomedicine*, 2012, 7, 1045-1066.

17. A. Palmquist, A. Johansson, F. Suska, R. Brånemark and P. Thomsen, *Clinical Implant Dentistry and Related Research*, 2013, 15, 96-104.

18. L. E. McNamara, R. J. McMurray, M. J. P. Biggs, F. Kantawong, R. O. C. Oreffo and M. J. Dalby, *Journal of Tissue Engineering*, 2010, 1.

19. Y. Wang, G. Subbiahdoss, J. Swartjes, H. C. van der Mei, H. J. Busscher and M. Libera, *Advanced Functional Materials*, 2011, 21, 3916-3923.

20. S. Sista, A. Nouri, Y. Li, C. Wen, P. D. Hodgson and G. Pande, *Journal of Biomedical Materials Research Part A*, 2013.

21. A. Cohen, P. Liu-Synder, D. Storey and T. J. Webster, *Nanoscale Research Letters*, 2007, 2, 385-390.

22. K. S. Brammer, S. Oh, C. J. Frandsen and S. Jin, *Biomaterials Science and Engineering ISBN*, 978-953.

23. H. Kenar, E. Akman, E. Kacar, A. Demir, H. Park, H. Abdul-Khaliq, C. Aktas and E. Karaoz, *Colloids and Surfaces B: Biointerfaces*, 2013, 108, 305-312.

24. C. J. Oates, W. Wen and D. W. Hamilton, *Materials*, 2011, 4, 893-907.

25. F. Rupp, L. Scheideler, D. Rehbein, D. Axmann and J. Geis-Gerstorfer, *Biomaterials*, 2004, 25, 1429-1438.

26. E. Eisenbarth, J. Meyle, W. Nachtigall and J. Breme, *Biomaterials*, 1996, 17, 1399-1403.

27. R. Xing, L. Salou, S. Taxt-Lamolle, J. E. Reseland, S. P. Lyngstadaas and H. J. Haugen, *Journal of Biomedical Materials Research Part A*, 2013, n/a-n/a.

28. K. Nakanishi, T. Sakiyama and K. Imamura, *Journal of bioscience and bioengineering*, 2001, 91, 233-244.

29. R. W. Mahley, *Science*, 1988, 240, 622-630.

30. P. G. W. Gettins, *Chemical Reviews*, 2002, 102, 4751-4804.

31. J. A. Sanz-Herrera, P. Moreo, J. M. García-Aznar and M. Doblaré, *Biomaterials*, 2009, 30, 6674-6686.

32. A. Khademhosseini, M. H. May and M. V. Sefton, *Tissue Engineering*, 2005, 11, 1797-1806.

33. M. D. Abràmoff, P. J. Magalhães and S. J. Ram, *Biophotonics international*, 2004, 11, 36-43.

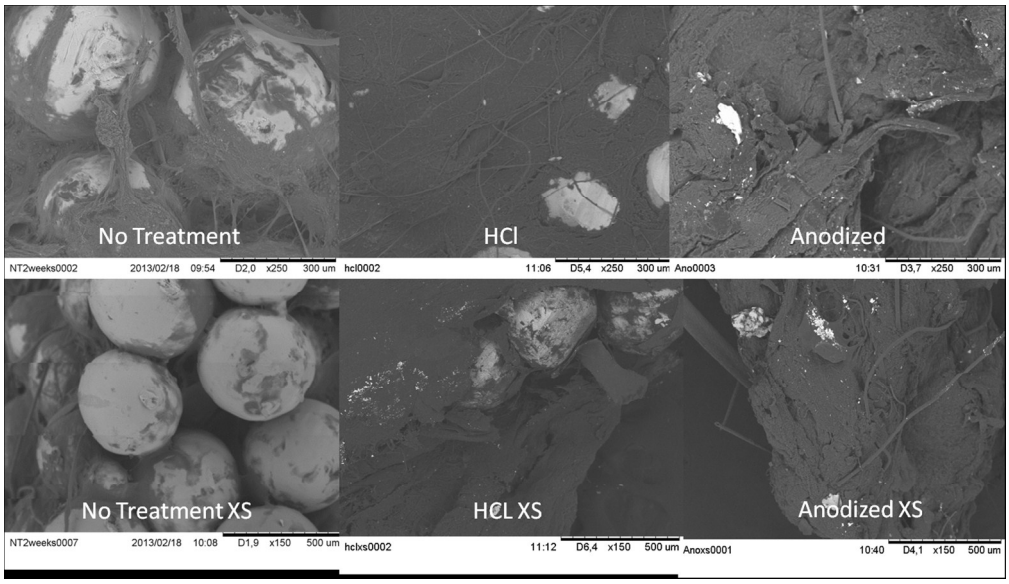

254x145mm (150 x 150 DPI)

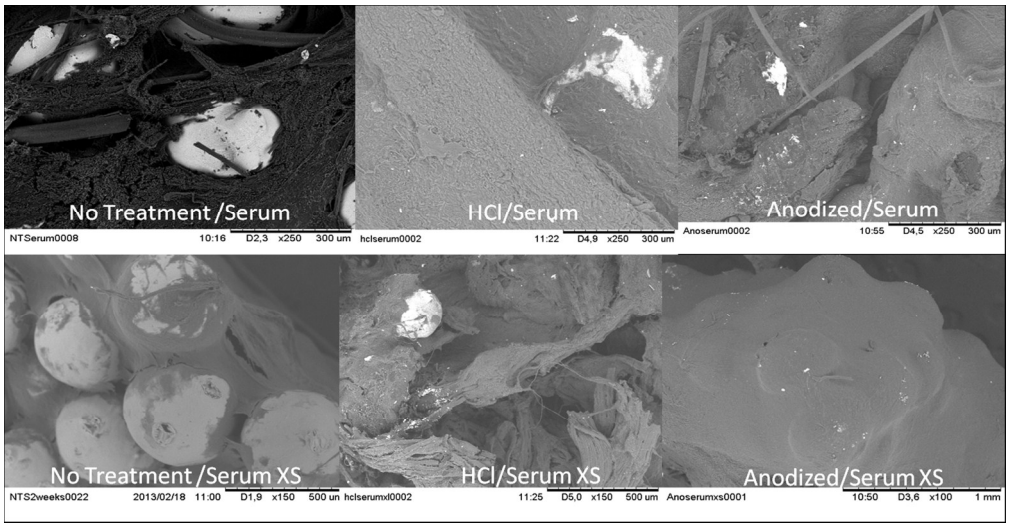

254x131mm (150 x 150 DPI)

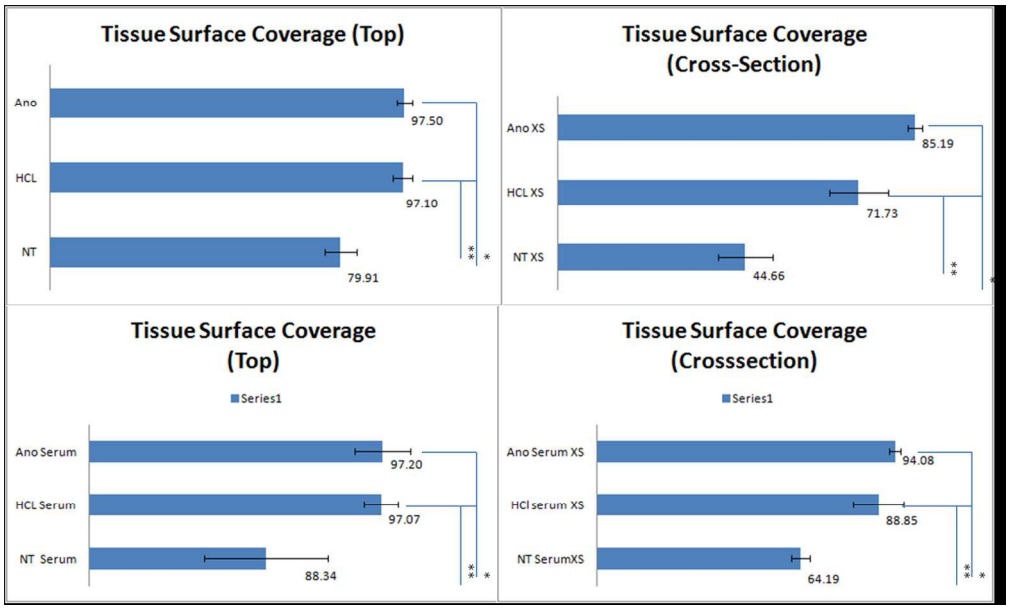

257x153mm (150 x 150 DPI)

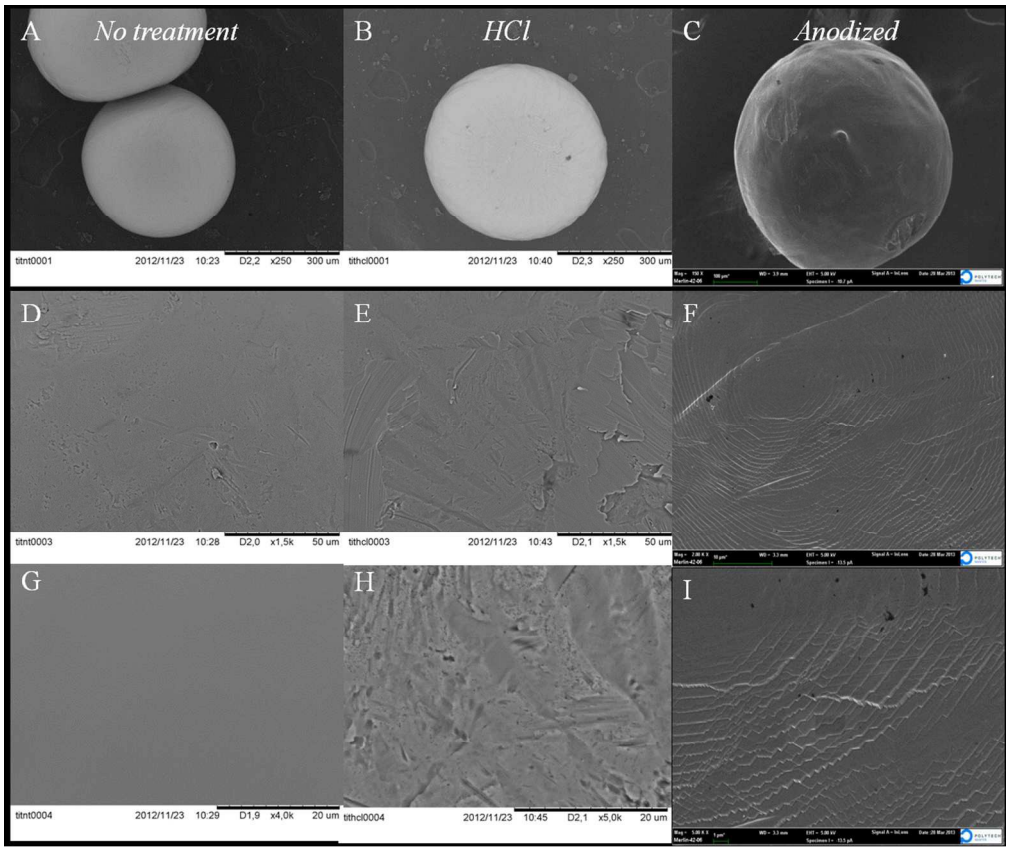

231x194mm (150 x 150 DPI)

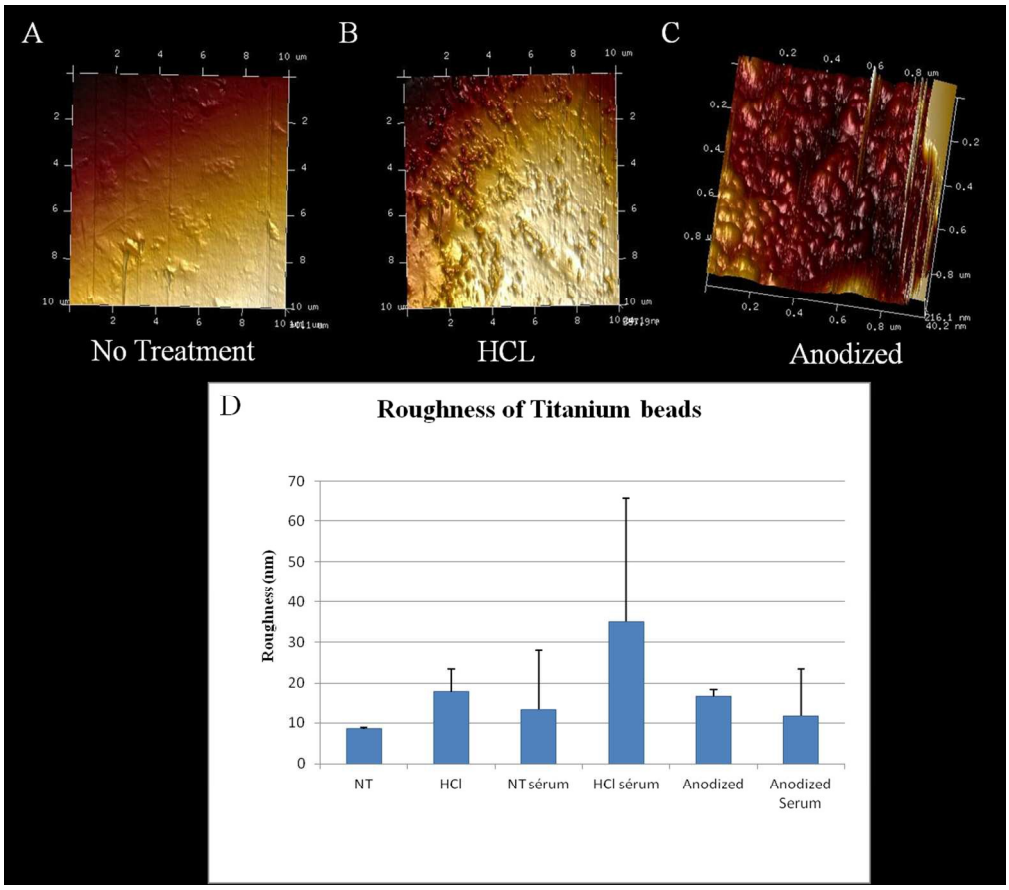

217x191mm (150 x 150 DPI)

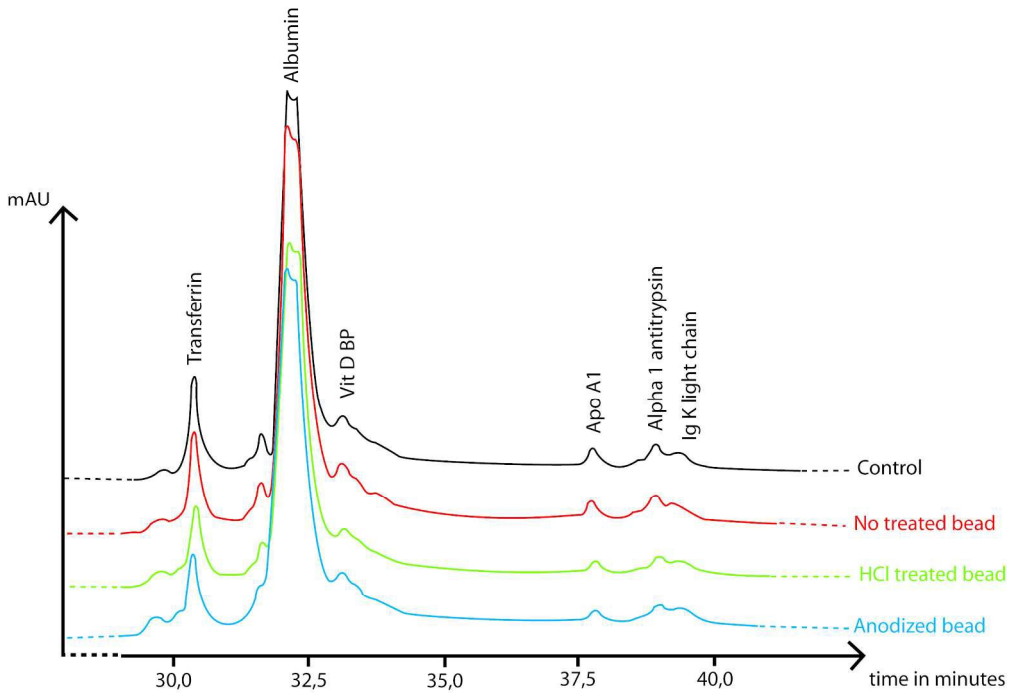

201x137mm (300 x 300 DPI)

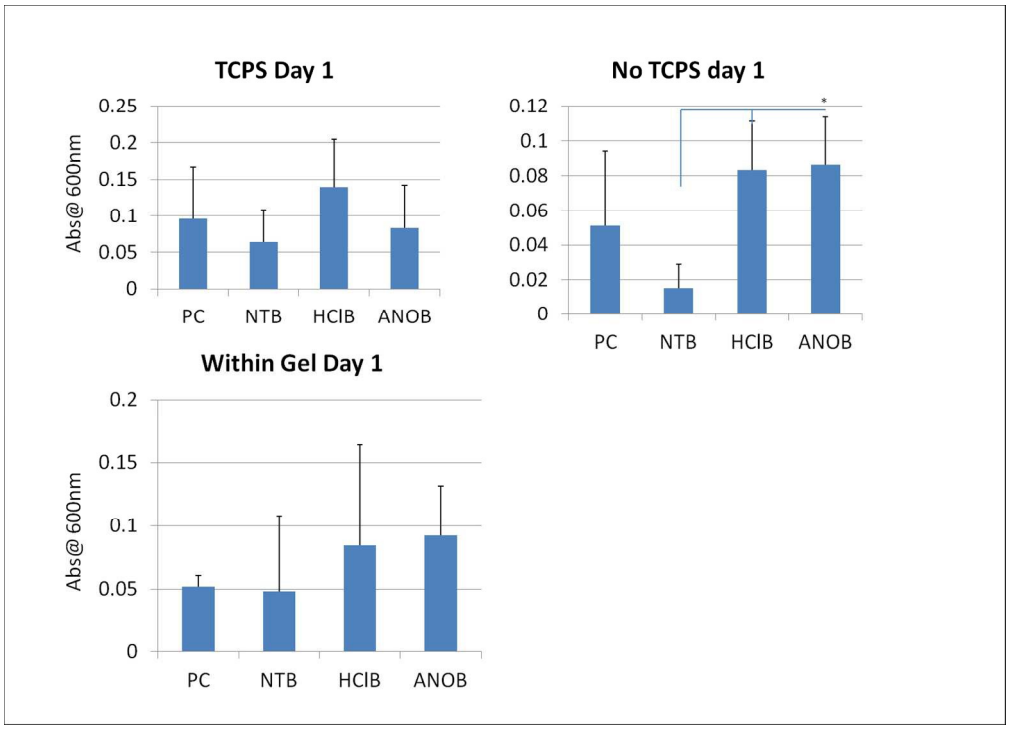

290x208mm (150 x 150 DPI)

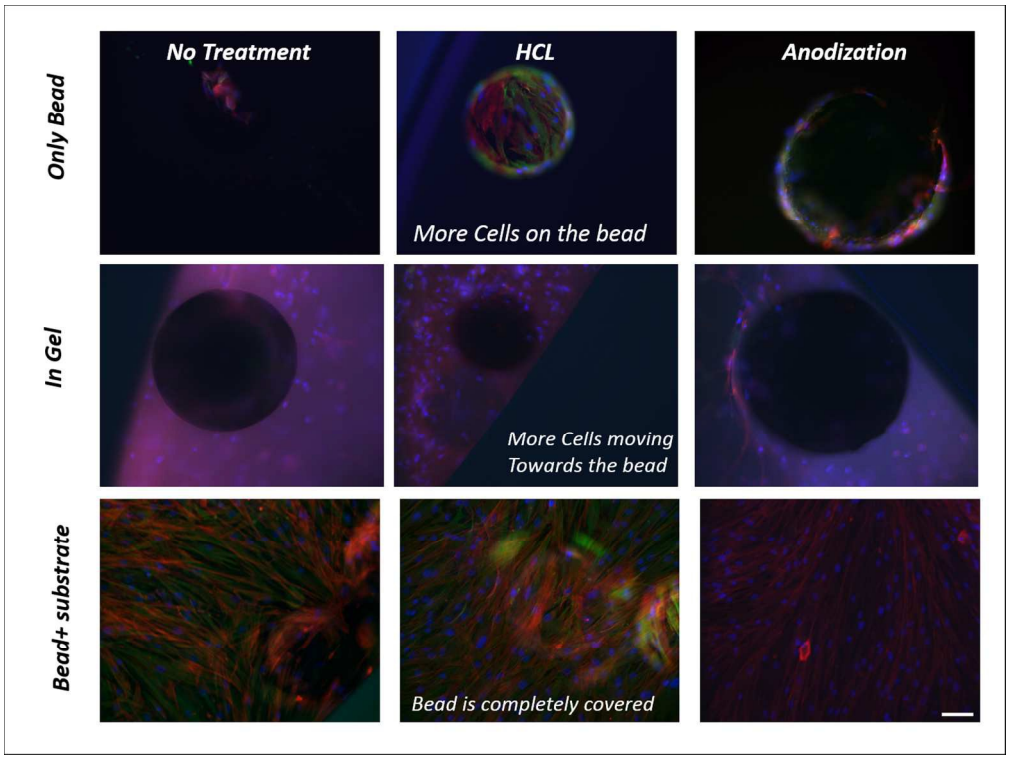

254x190mm (150 x 150 DPI)

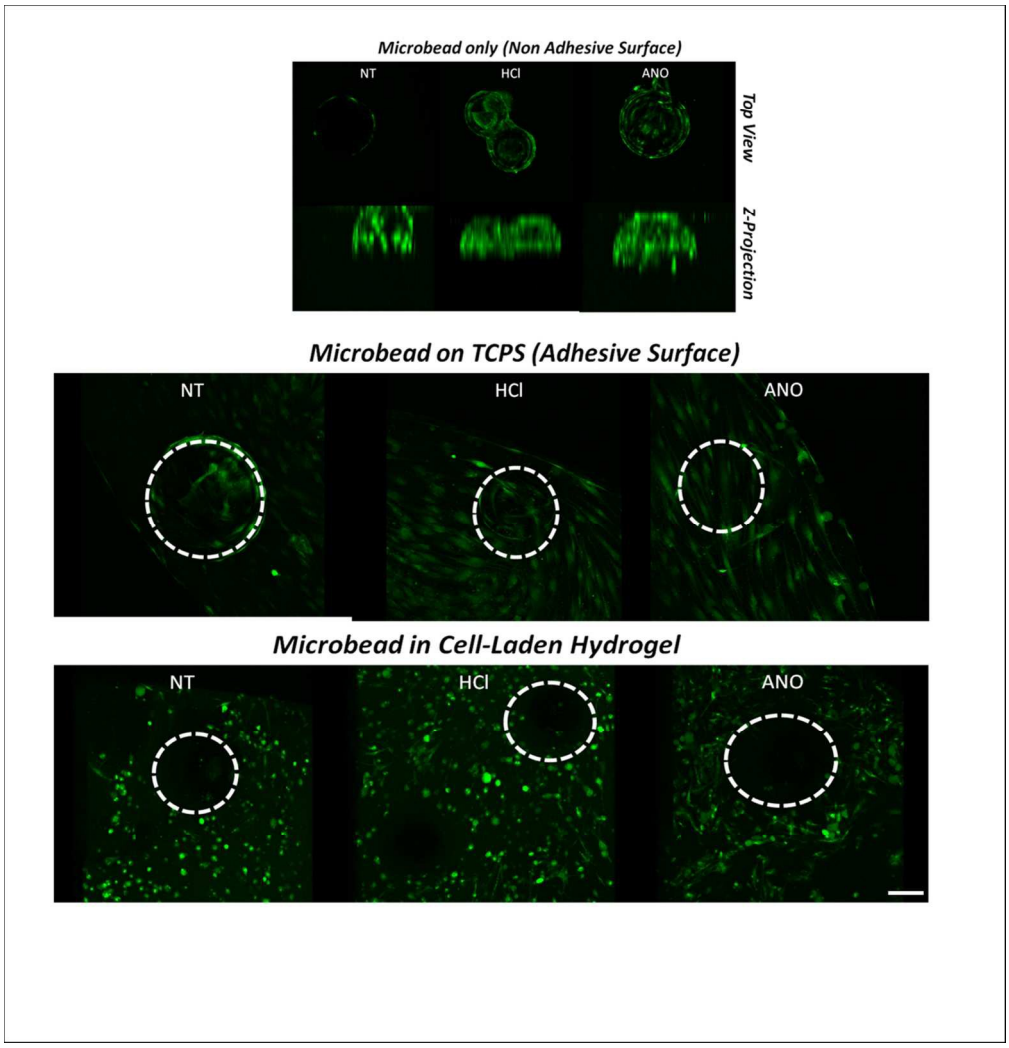

226x234mm (150 x 150 DPI)

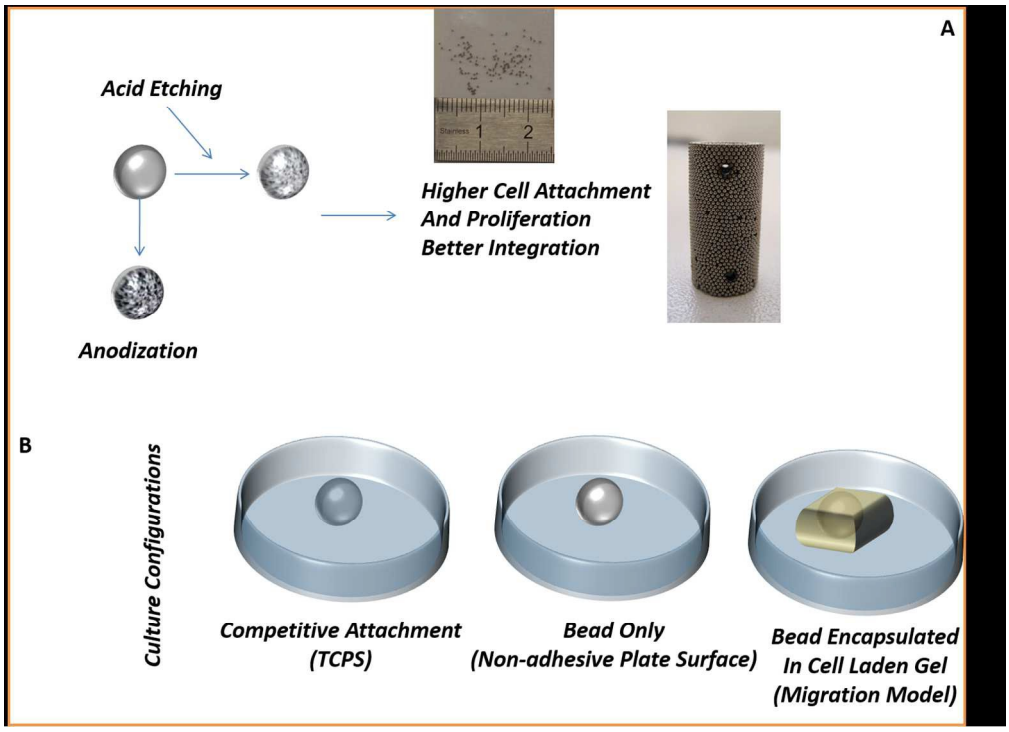

266x191mm (150 x 150 DPI)